

Control and Coherence of the Optical Transition of Single Nitrogen Vacancy Centers in Diamond

Lucio Robledo,* Hannes Bernien, Ilse van Weperen, and Ronald Hanson

Kavli Institute of Nanoscience Delft, Delft University of Technology, P.O. Box 5046, 2600 GA Delft, The Netherlands

(Received 27 May 2010; published 21 October 2010)

We demonstrate coherent control of the optical transition of single nitrogen-vacancy defect centers in diamond. On applying short resonant laser pulses, we observe optical Rabi oscillations with a half period as short as 1 ns, an order of magnitude shorter than the spontaneous emission time. By studying the decay of Rabi oscillations, we find that the decoherence is dominated by laser-induced spectral jumps. By using a low-power probe pulse as a detuning sensor and applying postselection, we demonstrate that spectral diffusion can be overcome in this system to generate coherent photons.

DOI: 10.1103/PhysRevLett.105.177403

PACS numbers: 78.47.jp, 42.50.Md, 61.72.jn, 78.55.Ap

Quantum control of light and matter is an outstanding challenge in modern science. Full control over both the spin state and the optical transition of a quantum system enables exciting applications such as spin-based quantum information processing and long-distance quantum teleportation of a spin state [1]. The basic operation underlying these applications, generation of nonlocal spin-spin entanglement, was recently demonstrated using individual trapped ions [2]. It is highly desirable to achieve the same level of control in solid-state systems as these may be easier to scale and promise higher integration density.

Candidate systems are required to have an electronic ground state with nonzero spin as well as a strong optical transition. Furthermore, coherent control over this transition is essential, as well as indistinguishability of the emitted photons [3]. In this context, several promising systems are studied extensively. Two-photon interference from independent sources was demonstrated for donor-bound excitons in semiconductors [4] and for quantum dots [5]. Optical Rabi oscillations have been observed in quantum dots [6] and nitrogen-vacancy (N-V) color centers in diamond [7]. A major challenge for these solid-state systems is the inhomogeneous broadening of the optical transitions caused by fluctuations in the solid-state environment [8–10]. These fluctuations not only degrade the fidelity of optical control, but also reduce the visibility in two-photon interference experiments. Since this interference is crucial for generating nonlocal entanglement, imperfect contrast directly translates into a reduced entanglement fidelity.

Here, we demonstrate coherent optical control over the orbital state of single N-V centers in diamond. Using short resonant laser pulses, we induce coherent oscillations of the optical transition. The decay of these oscillations yields important information on the transition's coherence [11]. We study the dependence of the coherence time on the involved laser fields. In particular, we find that spectral jumps, induced by an inevitable repump process, appear to degrade the fidelity of optical control. A scheme where

the control is preceded by a detuning-sensitive stage is implemented. We show that post-selection based on the detuning sensing can be used to circumvent the degrading effect of spectral jumps on two-photon interference.

The N-V center consists of a single substitutional nitrogen atom in the diamond lattice, located next to a vacancy. We use a type IIa bulk diamond sample from Element Six ($\langle 100 \rangle$ oriented, grown by chemical vapor deposition), containing a concentration low enough to detect individual negatively charged N-V⁻ centers [Fig. 1(a)].

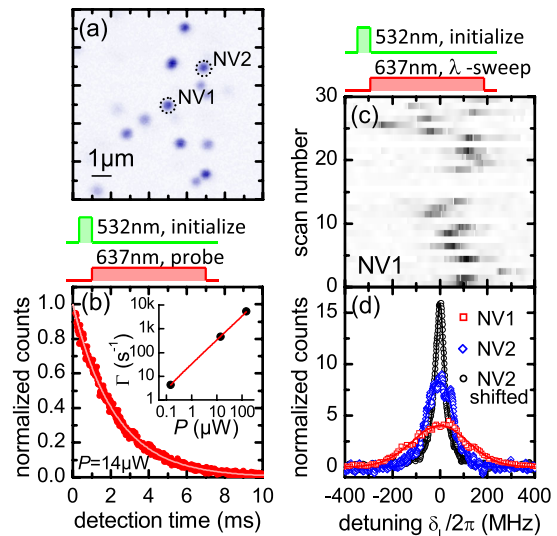


FIG. 1 (color online). (a) Confocal fluorescence image of individual N-V centers. (b) Resonant excitation leads to exponential decay of fluorescence due to photoionization. Inset: Ionization rate Γ as function of power of the resonant excitation laser. (c) Series of resonance scans. Green repump pulses applied in between scans to recharge the N-V center induce spectral jumps. (d) Sum of individual excitation scans yields frequency distribution of spectral jumps for NV1 and NV2. For comparison, for NV2 individual scans have been shifted to coincide in center frequency and then summed, to obtain the intrinsic linewidth. Data is normalized to the area under the curve.

The experiments are performed in a scanning confocal microscope using a flow cryostat at a temperature of $T = 8$ K. N-V center fluorescence is excited either off resonant using a $\lambda = 532$ nm (green) laser or on resonance by means of a narrow band tunable $\lambda = 637$ nm (red) diode laser. For continuous resonant excitation, the laser frequency is actively stabilized using a high-resolution wave meter. An electro-optical modulator with rise time of 1.3 ns allows us to apply short resonant pulses. The $\lambda = 532$ nm beam is sent through an acousto-optical modulator with a rise time of 4 ns. A dichroic mirror and additional longpass filters reject the excitation laser, so that only emission into the phonon sidebands (> 660 nm) is detected by an avalanche photodiode in the single-photon counting regime.

Excitation spectra are obtained by sweeping the excitation frequency across the N-V center resonance and recording the redshifted phonon-sideband emission. A spin triplet ground state with sublevels ($S_{x,y,z}$) and orbital A_2 symmetry, coupled to an excited state consisting of a spin triplet with sublevels ($S_{x,y,z}$) and orbital doublet with sublevels ($E_{x,y}$) gives rise to six resonances [12]. However, in general, strong spin-flip transitions lead to fast spin polarization, preventing most resonances to be directly observed in single-laser excitation experiments [13]. Here, we show results from N-V centers in the high strain regime ($\delta_{\text{str}} \approx 40$ GHz [14]) where we excite the cycling (S_z, A_2) \leftrightarrow (S_z, E_x) transition [13]. This transition has a very low probability for spin flips. After a spin flip the same laser field can excite the (S_x, A_2) \leftrightarrow (S_x, E_x) resonance detuned by ≈ 200 MHz which suffers from strong spin polarization back into the S_z state [12]. The effect of hyperfine interaction can be neglected at the time scale of our experiment [15]. In conclusion this transition represents a good approximation to a two-level system.

Continuous resonant excitation quickly bleaches N-V emission, which can be recovered by off-resonant green excitation. We measure the fluorescence decay rate as a function of resonant laser power by applying a pulse sequence that alternates a 10 μ s green pulse and 200 ms resonant excitation. We find that the fluorescence during the resonant pulse decays exponentially at a rate proportional to the driving power, provided the excitation power saturates the N-V transition [Fig. 1(b)]. The same decay is observed with and without simultaneous microwave excitation at 2.88 GHz, eliminating spin polarization as a possible explanation. Excitation at $\lambda = 637$ nm, but detuned from the exact resonance, does not bleach the N-V center. These results indicate that photo-ionization of the center out of the excited state is the origin of the observed decay [16]. Off-resonant (green) excitation can excite charge impurities in the environment of the N-V center (e.g., substitutional nitrogen [17]) which can bring the N-V center back to the negative charge state. This mechanism is intrinsic to the N-V center, and explains the need for off-resonant repumping whenever driving N-V centers resonantly.

Figure 1(c) shows a series of resonant excitation scans. Between each scan, a green pulse was applied to prepare the N-V center in the negative charge state and initialize the spin into the S_z state [12]. Large spectral jumps from scan to scan and occasional photoionization can be observed. In absence of the green pulse, spectral jumps remain below our experimental resolution (however the probability of ionization increases). This observation is consistent with the assumption that the green laser changes the local charge environment, leading to a shift of the resonance frequency via the DC Stark effect. The distribution of spectral jumps is thus dominated by the concentration of charge impurities in a center's direct environment. We observe large differences from center to center: In Fig. 1(d), we compare the range of jumps for two centers. Spectral jumps of NV1 occur over a twice as large range as those of NV2, suggesting a higher concentration of nearby charge impurities. Summing individual scans while compensating for the spectral jumps reveals the Lorentzian-shaped absorption line in the absence of green excitation. We find an intrinsic linewidth of 46 ± 2 MHz for both NV1 (data not shown) and NV2, presumably limited by interaction with the phonon bath at $T = 8$ K [18].

In order to achieve coherent control, we apply resonant pulses. The sequence consists of a 10 μ s green pulse to initialize the N-V⁻ charge and spin state, followed by 1000 repetitions of a 30 ns resonant laser pulse and a 70 ns off time to allow the N-V center to relax to its ground state before the next excitation cycle starts. We use a time-resolving, single-photon counter to histogram the photon detection time relative to the start of the resonant laser pulse with a bin size of $\Delta t_{\text{bin}} = 256$ ps. To build up statistics we sum over typically 10^9 pulses. The number of counts during a time bin is then proportional to the probability to occupy the excited state [19].

During a resonant laser pulse, we observe coherent oscillations between the N-V orbital states [Fig. 2(a)]. On resonance, the oscillation frequency is given by $\Omega_0 = \vec{\mu} \cdot \vec{E}/\hbar$, with $\vec{\mu}$ denoting the N-V zero-phonon-line dipole moment and \vec{E} the electric field vector. The resulting square root dependence of oscillation frequency on excitation power is clearly observed [Fig. 2(b)]. For the largest applied driving power, we can resolve > 10 oscillations. The obtained Rabi frequency of $\Omega = 2\pi \times 410$ MHz corresponds to a π pulse in only $t_\pi = 1.2$ ns.

The oscillations are damped due to spontaneous emission and additional dephasing, such as phonon scattering. Experimental data fits excellent to an exponentially damped harmonic oscillation $\cos[\Omega(t - t_0)] \times \exp[-(t - t_0)/\tau]$. On resonance, the exponential damping constant τ of the Rabi oscillations is determined by the pure dephasing time T_2^* via $1/\tau = 3/(4T_1) + 1/(2T_2^*)$ [20]. After turning off the driving field, the fluorescence decays exponentially due to spontaneous emission $\propto \exp(-t/T_1)$ with a lifetime T_1 of 10.9 ns.

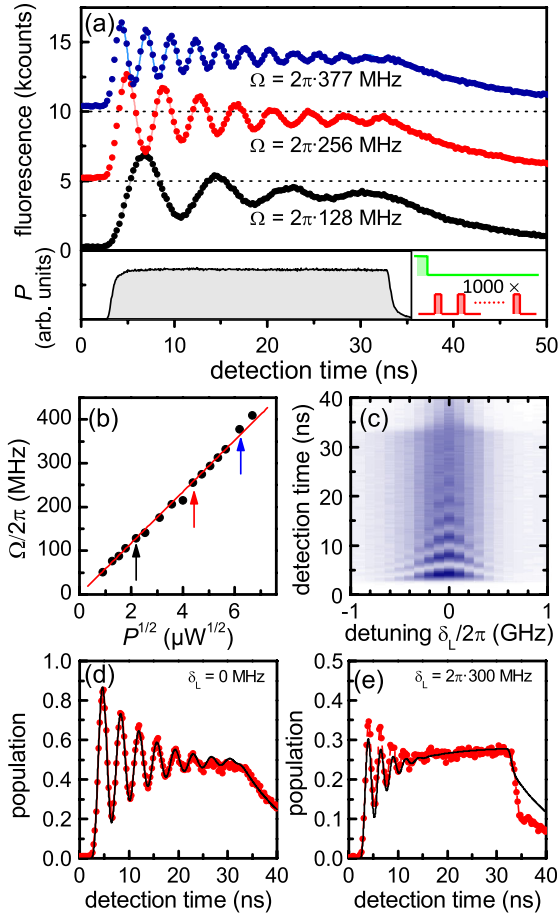


FIG. 2 (color online). (a) Rabi oscillations for $P = 38 \mu\text{W}$, $P = 19 \mu\text{W}$, and $P = 4.7 \mu\text{W}$. The lowest data set indicates the shape of the excitation pulse. (b) Rabi frequency plotted versus square root of excitation power. (c) Rabi oscillations as function of detuning for $\Omega_0 = 2\pi \times 272 \text{ MHz}$. (d),(e) Comparison of measured Rabi oscillations on resonance (d) and 300 MHz detuned (e), and numerical data obtained from numerically integrating the optical Bloch equations.

In Fig. 2(c) we show Rabi oscillations for NV2 as function of laser detuning δ_L . For detuned excitation the oscillation frequency increases to the generalized Rabi frequency $\Omega = \sqrt{\Omega_0^2 + \delta_L^2}$, while the oscillation amplitude decreases $\propto \Omega_0^2/(\Omega_0^2 + \delta_L^2)$ [21]. To accurately reproduce our experimental transients we numerically integrate the optical Bloch equations [Figs. 2(d) and 2(e)] [21], taking into account finite rise and fall times of the driving field, and applying a spectral average over a Gaussian distribution of detuning values of FWHM $b = 2\pi \times 40 \text{ MHz}$. We assume a pure dephasing time of $T_2^* = 10 \text{ ns}$, consistent with the observed linewidth of $\Delta = 46 \text{ MHz}$. The same simulation parameters are used to model the on resonance as well as the 300 MHz detuned transient. This simulation reproduces features for the detuned transients beyond the exponentially damped cosine, such as (i) the offset of the oscillations which increases with a negative exponential, (ii) the pronounced kink

arising from the state vector adiabatically following the detuned field vector during the finite fall time of our excitation pulses, and (iii) an increased damping rate [21].

In Fig. 3(a) we show the observed damping constant of Rabi oscillations on NV1 and NV2 as function of the Rabi frequency. Coherence of Rabi oscillations is ultimately limited by fast dephasing processes on a nanosecond time scale, such as phonon scattering [18]. However, for measurements that sum over several excitation cycles, such as the one in Fig. 2(a), we expect to be limited by slow processes such as the spectral jumps observed in Fig. 1(c). The total measurement represents an average over different detuning values and thus different Rabi frequencies, which leads to a faster damping of the observed oscillations. Consequently, for NV2 we observe a better coherence than for NV1. For Rabi frequencies much larger than the spectral width of the distribution of resonances, the deteriorating effect of spectral jumps vanishes, since the Rabi frequency always largely exceeds the detuning. This is apparent in the initial increase of τ for NV2 which quickly settles to about 9 ns for $\Omega > 2\pi \times 200 \text{ MHz}$. This value is close to the coherence expected from the linewidth [dashed line in Fig. 3(a)].

Previous research [7] suggested a decrease of coherence with increasing driving power. To investigate possible influence of the red laser on the coherence which is not related to the N-V center resonance, we measured the damping of Rabi oscillations while also shining a detuned ($\lambda = 640 \text{ nm}$) red laser onto the same N-V center [Fig. 3(b)]. Even at an excitation power 1 order of magnitude larger than used for driving optical Rabi oscillations, we see no significant effect of the off-resonant laser. We conclude that for N-V centers, optical coherence is not intrinsically limited by off-resonant effects of the driving field itself.

Summarizing these findings, the contrast of two-photon interference using N-V centers will primarily be limited by frequency fluctuations of the emitted photons. We make use of the slow time scale of these fluctuations to show that even for N-V centers suffering from unstable lines, the

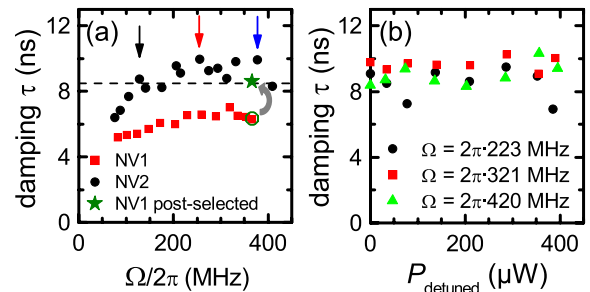


FIG. 3 (color online). (a) Damping constant τ of Rabi oscillations as function of Rabi frequency. The dashed line indicates limit of τ for T_2 set by the single-scan linewidth $\Delta = 48 \text{ MHz}$. Coherence is limited by spectral jumps (note difference between NV1 and NV2). Postselection can remove deteriorating effects of spectral jumps and enhance τ to the value expected from the linewidth. (b) An additional laser field at $\lambda = 640 \text{ nm}$ is applied: This detuned laser has no influence on coherence.

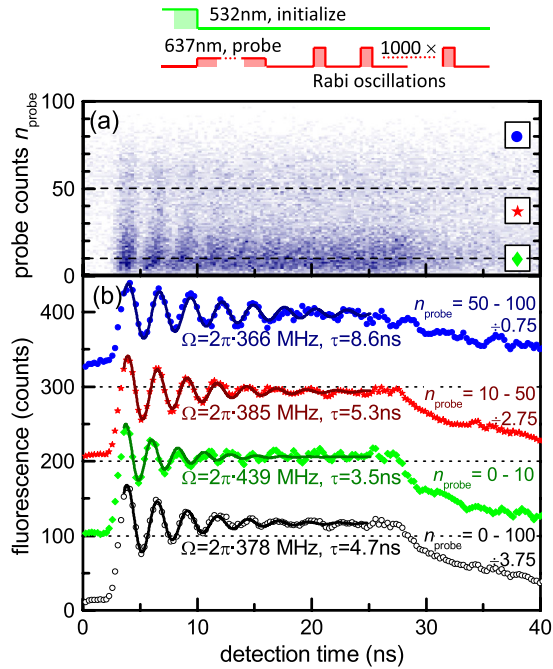


FIG. 4 (color online). (a) Detuning-resolved Rabi oscillations: detuning from resonance is derived from fluorescence counts during a 20 ms weak resonant probe pulse. Subsequently measured Rabi oscillations are plotted as function of this count rate. Total data is obtained from 3×10^7 excitation cycles. (b) Data from plot (a) is summed within three ranges. On-resonance (high counts during probe pulse) oscillations show lower Rabi frequency and increased coherence. Transients have been scaled by the indicated factor for better comparison.

spectral stability (i.e., the coherence time) set by the single-scan linewidth can be reached. For that purpose we modify our measurement protocol: after each green initialization pulse we introduce an additional (weak) resonant laser pulse of $t = 20$ ms and count the photons n_{probe} detected during that interval. These counts n_{probe} now serve as a measure of the laser detuning during that specific interval. For large detuning we expect low n_{probe} , while resonance is identified by a large value of n_{probe} . We then record the time-resolved fluorescence during the strong (Rabi) pulses as a function of n_{probe} [Fig. 4(a)]. The measured data is divided into three regions of n_{probe} and each of them is summed [Fig. 4(b)]. For low n_{probe} we identify the characteristic features of detuned excitation, as already observed in Fig. 2(e): increased Rabi frequency, increased damping, and a kink at the falling edge of the driving pulse. Postselecting on-resonance events in turn leads to improved coherence: Already the damping time of the intermediate region of n_{probe} outperforms the value for the overall data. Strikingly, selecting only the events with highest n_{probe} , the damping time is nearly doubled, and reaches the value expected from single-sweep linewidth measurements [Fig. 3(a)]. This scheme therefore allows for heralded two-photon interference for emitters with unstable resonances, provided that spectral jumps happen

on a time scale which is slow compared to the photon detection rate. Compared to an interference experiment based on spectral filtering of the emission lines of both emitters to ensure resonance, this scheme yields higher interference contrast as detector dark counts only need to be accumulated while emitters are resonant to the driving field.

In summary, we demonstrated coherent control over the N-V center's orbital state. Rabi frequencies $\Omega > 2\pi \times 400$ MHz with more than 10 oscillations have been observed. Damping of Rabi oscillations is dominated by slow spectral jumps of the N-V's resonance frequency, which, however, can be overcome by a detuning-sensitive stage prior to coherent control. This result highlights the good prospects for quantum information processing based on probabilistic entanglement of distant N-V centers using two-photon interference.

We thank V. V. Dobrovitski, F. Jelezko, and M. D. Lukin for fruitful discussions. This work is supported by the Dutch Organization for Fundamental Research on Matter (FOM) and the Netherlands Organization for Scientific Research (NWO). L.R. acknowledges support of the European Community under a Marie Curie IEF Action.

*l.m.robledoesparza@tudelft.nl

- [1] S. Olmschenk *et al.*, *Science* **323**, 486 (2009).
- [2] D. L. Moehring *et al.*, *Nature (London)* **449**, 68 (2007).
- [3] C. K. Hong, Z. Y. Ou, and L. Mandel, *Phys. Rev. Lett.* **59**, 2044 (1987).
- [4] K. Sanaka *et al.*, *Phys. Rev. Lett.* **103**, 053601 (2009).
- [5] R. J. Patel *et al.*, *Phys. Rev. Lett.* **100**, 207405 (2008).
- [6] T. H. Stievater *et al.*, *Phys. Rev. Lett.* **87**, 133603 (2001).
- [7] A. Batalov *et al.*, *Phys. Rev. Lett.* **100**, 077401 (2008).
- [8] Ch. Santori *et al.*, *Nature (London)* **419**, 594 (2002).
- [9] A. Högele *et al.*, *Phys. Rev. Lett.* **93**, 217401 (2004).
- [10] F. Jelezko *et al.*, *Appl. Phys. Lett.* **81**, 2160 (2002).
- [11] S. Kummer, S. Mais, and Th. Basché, *J. Phys. Chem.* **99**, 17078 (1995).
- [12] N. B. Manson, J. P. Harrison, and M. J. Sellars, *Phys. Rev. B* **74**, 104303 (2006).
- [13] Ph. Tamarat *et al.*, *New J. Phys.* **10**, 045004 (2008).
- [14] To determine the strain splitting, we measured the excitation spectrum of NV1 consisting of six resonances. Simultaneous microwave excitation resonant with the ground state splitting of 2.88 GHz was used to prevent spin polarization. All shown data has been obtained without additional microwave excitation.
- [15] P. Neumann *et al.*, *Science* **329**, 542 (2010).
- [16] N. B. Manson and J. P. Harrison, *Diam. Relat. Mater.* **14**, 1705 (2005).
- [17] F. J. Heremans *et al.*, *Appl. Phys. Lett.* **94**, 152102 (2009).
- [18] K.-M. C. Fu *et al.*, *Phys. Rev. Lett.* **103**, 256404 (2009).
- [19] I. Gerhardt *et al.*, *Phys. Rev. A* **79**, 011402(R) (2009).
- [20] W. E. Moerner, M. Orrit, and U. Wild, T. Basché, *Single Molecule Optical Detection, Imaging and Spectroscopy* (Wiley-VCH, Weinheim, 1996).
- [21] L. Allen and J. H. Eberly, *Optical Resonance and Two-Level Atoms* (Dover, New York, 1987).